

## Using FEEM-PARAFAC to characterize metabolic organic components from P17 and NOX strains after AOC assay

Hsiao-Jung Ho<sup>a</sup>, Jing-Wen Cao<sup>b</sup>, Chih-Ming Kao<sup>a</sup>, Wen-Liang Lai<sup>b,\*</sup>

<sup>a</sup>*Institute of Environmental Engineering, National Sun Yat-Sen University, 70 Lienhai Road, Kaohsiung 80424, Taiwan, ROC, emails: d023030002@student.nsysu.edu.tw (H.-J. Ho), jkao@mail.nsysu.edu.tw (C.-M. Kao)*

<sup>b</sup>*Graduate School of Environmental Management, Tajen University, 20 Weixin Road, Yanpu Township, Pingtung 90741, Taiwan, ROC, Tel. +886-8-762-4002 Ext. 2607; emails: lai@tajen.edu.tw (W.-L. Lai), machihisoka@hotmail.com (J.-W. Cao)*

Received 10 September 2018; Accepted 27 March 2019

---

### ABSTRACT

Fluorescence excitation-emission matrices (FEEMs) and parallel factor analysis (PARAFAC) techniques are able to evaluate the chemical characteristics of overlapping fluorophores and bands in FEEM. In this study, FEEM-PARAFAC was applied to distinguish the differences among metabolic organic components from *Pseudomonas fluorescens* P17 and *Spirillum* NOX strains in an assimilable organic carbon bioassay with acetate as the primary substrate. Three metabolic components from P17 and NOX strains were selected and grown in different acetate concentrations based on the simultaneous consideration of verification of variance, core consistency, residuals, and split-half experiments. The results from control tests show that metabolic humic-like substances in the NOX strain were more prevalent than they were in the P17 strain. Metabolic humic-like substances from the P17 strain increased with escalating acetate concentrations, while a descending trend occurred in experiments with the NOX strain, indicating that the composition of metabolic organic matter containing nitrogen and humic-like substances varied according to the acetate concentrations.

*Keywords:* Assimilable organic carbon; Dissolved organic matter; *Pseudomonas fluorescens* P17; *Spirillum* NOX strains

---

### 1. Introduction

Inside water supply distribution systems, heterotrophic bacteria in the bulk solution utilize available substrates as a source of carbon, nutrients, and energy. Regrowth of bacteria can not only accelerate corrosion and lower hydraulic capacity but also cause the difficulty of maintaining a disinfection residual in the distribution system [1]. Changing flow conditions in the network could result in proliferation of microorganisms on pipe surfaces, especially pathogenic species. Biodegradable organic matter (BOM) has been demonstrated to be one of the major factors in accelerating microbiological growth in distribution systems [2]. Part of the dissolved organic matter (DOM) was contrasted with the nonbiodegradable fraction based on the operational

definition of the measurement of BOM characterization. BOM could serve as an energy and carbon source for the metabolic processes of heterotrophic bacteria [3]. Consequently, BOM removal in water treatments is a concerning factor for the following reasons: (1) it is easily utilized by microbial regrowth in the distribution system; (2) formation of disinfection by products (DBPs) by its reaction with chlorine oxidant; and (3) the specific contaminants which are unfavorable for health [4].

The common measurements of BOM are divided into biodegradable organic carbon (BDOC) and assimilable organic carbon (AOC) under aerobic conditions [2]. Based on the bacterial elemental composition of the C:N:P ratio, the extent of bacterial growth is governed by the concentrations of available organic and inorganic nutrients. Although some research on BOM substrates (e.g., formaldehyde, geosmin, biodegradable humic substances) have identified

---

\* Corresponding author.

specific biodegradable organic compounds [3], few papers pay attention to this characteristic of metabolic organic matter from anaerobic bacteria incubated for the measurement of BOM [1].

The BOM level varied with the source water for drinking water treatments from natural or anthropogenic organic matter. Oxidation processes, such as disinfectant addition, especially for ozone processes in water treatments, could affect the content of the available substrate for bacterial utilization due to the formation of low molecular weight compounds from the reaction of residual disinfectants with natural organic matter (NOM) [5]. Sequentially, bacterial community composition was significantly shifted. Meanwhile, another issue mentioned by Li et al. [5] should give attention: the growth of nitrifying bacteria in distribution systems resulting from monochloramine disinfectants.

Regarding the NOM characteristic in varied aquatic ecosystems, heterogeneous and unclear mixtures of divergent aliphatic and aromatic compounds with a broad range of molecular weights have been investigated by the research of Goslan et al. [6]. Composition and characteristics of the aquatic NOM were related with the original sources and sequentially affected by physical, chemical and biological processes including water chemistry, environmental conditions of temperature and pH, and biological activities [7]. Actually, different properties as well as the organic concentration could affect the operational efficiency of water treatment processes, the consumption of coagulant dosage, and the formation of potentially harmful DBPs such as trihalomethanes and haloacetic acid, especially those with higher aromaticity, molecular weight, and hydrophobicity [8,9].

Reproducible methods for NOM characterization were important for the evaluation of the operational efficiency of drinking water treatment [10]. Traditional techniques for the analysis of NOM characteristics include total organic carbon (TOC) instrumental analysis, color, and UV absorbance spectroscopy [11]. TOC represents nothing pertaining to the organic properties besides the information regarding the concentration. Similarly, color restricts the indication of the concentration of humus substances such as the humic and fulvic fractions [12], but the UV absorbance coefficient at 254 nm divided by TOC content, referred as SUVA, could indicate the degree of the aromaticity of NOM [13].

Recently, optical instruments including absorbance and fluorescence have been widely applied in the investigation of the changes in composition and concentration of organic matter [14]. These optical measurements have proven to represent sensitive indexes of the complex DOM mixture with applicable ability to track subtle changes in water quality [15]. DOM fluorescence is a sensitive tracer correlated with *Escherichia coli* abundance in sewage [16]. Fluorescence spectroscopy could be easily implemented in both field and lab-scale operation situations; furthermore, reduced expense versus liquid chromatography and nondestructive techniques could enable rapid clustering of DOM fractions according to their chemical properties [17]. Beggs and Summers [18] have proven that fluorescence spectroscopy is an available tool for determining DOM characteristics, functional groups and relative amounts of organic matter, especially for the rapid acquisition of 3D fluorescence excitation-emission matrices (FEEMs) represented by contour

maps with excitation and emission wavelengths, as well as fluorescence intensity. Consequently, the complex DOM can be classified by its fluorescent components (fluorophores). However, the quantification of the total amount of organic matter for each fraction is still not solved, indicating that previous calibration should be conducted [19].

For elucidating immense data in 3D-FEEM, developed methods included the traditional peak picking method [20], fluorescence regional integration [21], multivariate data analysis [22], parallel factor framework-clustering analysis [23], and multiway data analysis using parallel factor analysis (PARAFAC) [14]. For the peak-picking method, it was regarded as a simple tool to identify the corresponding excitation and emission wavelength pairs of components based on their maximum intensity [24], and even real-time tools with available sensors have been developed by the peak-picking technique. However, its limited applicability may be related with misleading observations due to the phenomena of the shifts, overlapping, and interferences from peak components [25].

Refined techniques for data interpretation of FEEM, from simple methods such as peak-picking to more complex methods such as principal component analysis (PCA), PARAFAC and self-organizing maps, were developed for solving potentially misleading observation. PCA uses a statistical procedure to reduce the number of variables, but it preserves most of the relevant information [26]. PARAFAC, applied with advanced data processes, decomposes the fluorescence spectra into a set of unique components [27].

Multiway analytical techniques, particularly PARAFAC, have been considerably applied into FEEM analysis in marine, natural aquatic body and groundwater environments as well as in wastewater, recycled and drinking water systems [28–33]. PARAFAC can separate the contributions of different fluorophores without additional assumptions about their excitation and emission spectra, which provides meaningful information regarding the major components from organic FEEMs diagrams [25,34]. However, the complex postprocessing of PARAFAC analysis limits the wider applications of FEEM spectroscopy on DOM monitoring. A detailed description of the PARAFAC method with respect to components in wastewater has been reported by Yang et al. [25], even proposing that PARAFAC could be developed into a surrogate method for determining conventional water quality parameters and the treatability of NOM by treatment processes.

According to the results of previous studies [25,34], FEEM analysis using the peak-picking method was constrained and misunderstood due to the phenomena of shifts, possible overlapping and interferences of peaks. In contrast, the PARAFAC tool can effectively separate the contribution of different fluorophores without additional assumptions about their excitation and emission spectra, resulting in meaningful information regarding major components from FEEM diagrams. Consequently, in this study, the metabolic organic characteristics from P17 and NOX strains in the AOC bioassay were elucidated with FEEM and PARAFAC for distinguishing the differences among major metabolic components and understanding the effect of acetate concentrations (used as primary substrates) on the production of major components.

## 2. Materials and methods

### 2.1. Incubation of P17 and NOX

Standard acetate concentrations of control test (without acetate-C), 10 and 100 µg acetate-C/L were prepared from a stock sodium acetate solution diluted with a volume of 600 mL of diluted water from groundwater treated with quartz sand, granular activated carbon, cation exchange resin, and reverse osmosis (RO) processes. Each standard solution was supplemented with 0.4 mL of 0.0026 M  $K_2HPO_4$  for maintaining the constant phosphate amounts. The substrate and phosphate contained in solution were respectively added for the incubation of *Pseudomonas fluorescens* P17 and *Spirillum* sp. NOX incubation according to the procedures described in Van der Kooij and Veenendaal [35]. The initial colony number was closely maintained at 300 CFU/mL after inoculation.

### 2.2. FEEM measurements

Whole samples were filtered through 0.22 µm cellulose membranes (mixed cellulose ester, Advantec, Japan) prior to the operation of a fluorescence spectrometer (F-4500, Hitachi, Japan) with 1 cm quartz cuvettes. FEEM scans were controlled within the range of 200 to 600 nm for both emission (Em) and excitation (Ex) wavelengths with 10 nm increments, 12,000 nm/min scan speed, and 10 nm Ex/Em slit bandwidths. The interference of blank fluorescence spectra induced from Milli-Q water was subtracted from whole FEEM samples. Built-in software within the instrument could effectively eliminate Raman and Rayleigh scattering effects.

### 2.3. Transformation of FEEM dataset and the criterion of PARAFAC operation

Trilinear data, transformed from three dimensional datasets of FEEMs, can be constructed as the sum of a limited

number of independently varying fluorescence signals [36]. Outlier samples resulting in analytical errors can be identified through examining the influences of both sample and wavelength on a model. These independent signals, components with relative concentrations in each sample, can be quantified by the PARAFAC algorithm to identify the best-fitting excitation and emission spectra. In this research, FEEM fluorescence data were obtained using the DOMFluor Toolbox in MATLAB 2017a (Mathworks, Natick, MA) with the detailed operational procedure described by the report of Stedmon and Bro [37]. Usually, 2 and 5 components were generated by an integrated validation method including variance explanation, core consistency diagnosis, half split analysis, and residual and visual inspection [14].

## 3. Results and discussion

### 3.1. Determination of N components

Shimotori et al. [38] proved that the composition of fluorescent dissolved organic matter (FDOM) depended on the bacterial taxonomic groups, demonstrating that 10 among 14 peaks produced from 11 cultures of isolated bacterial strains showed different fluorescence characteristics. Therefore, PARAFAC modeling applied to FEEMs of metabolic organic products measured from P17 and NOX strains for measuring AOC content was conducted in this study. The major identified components pertaining to excitation-emission location and fluorescence intensity have been linked to the characteristic and to the changes of fluorescent DOM content [28,39].

According to a previous survey, the determination of components could be judged from explained variance, core consistency, and residuals [14], as listed in Table 1. Sample numbers for the P17 strain and NOX strain were 6 and 5, respectively, for each substrate concentration. As observed

Table 1

Summary of factors (F) of PARAFAC model responding to sum-of-squares of residuals, explained variation, and core consistency (sample numbers of 6 for P17 strain and 5 for NOX strain for each substrate concentration)

Substrate (µg acetate-C/L)	Factors	Sum-of-squares of residuals		Explained variation (%)		Core consistency (%)	
		P17	NOX	P17	NOX	P17	NOX
Control	2	1020929.52	7690638.52	82.84	87.48	99.92	95.76
	3	375794.26 (63.2%)*	3904539.73 (49.2%)	93.68	93.64	57.65	94.34
	4	250076.20 (33.5%)	2724672.44 (30.2%)	95.79	95.56	74.39	44.36
	5	213003.64 (14.8%)	2463264.17 (9.6%)	96.42	95.99	9.35	20.90
10	2	477830.21	3895223.45	89.94	88.77	99.43	99.02
	3	235868.74 (50.6%)	2294876.32 (41.1%)	95.04	93.39	82.05	95.43
	4	173512.17 (26.4%)	1431579.20 (37.6%)	96.35	95.87	78.19	41.73
	5	118397.43 (31.8%)	1045046.93 (27.0%)	97.51	96.98	24.25	24.41
100	2	813223.72	2338509.29	92.12	89.13	99.97	99.46
	3	525965.76 (35.3%)	1484771.86 (36.5%)	94.90	93.09	92.00	94.71
	4	316455.61 (39.8%)	963955.32 (35.1%)	96.93	95.52	55.55	18.81
	5	258797.86 (18.2%)	670551.47 (30.4%)	97.49	96.88	5.93	2.36

\*(Sum-of-Squares of residuals in previous component - Sum-of-Squares of residuals in later component)/Sum-of-Squares of residuals in previous component.

from Table 1, the core consistency values of PARAFAC modeling for metabolic organic content from the P17 strain control test decreased from the maximal value of 99.92%, with the factor of 2, to the lowest value of 9.53% with the factor of 5. The switch point of core consistency value occurred at the factor of 3. Regarding the core consistency values of PARAFAC modeling for metabolic organic content from the NOX strain, the value of 95.76% with factor 2 decreased to 20.96% with the factor of 5. The maximal shift point occurred with the factor of 3. Based on the adherence of the PARAFAC algorithm [14], the suitable number of PARAFAC components for each P17 and NOX strain should be simultaneously suggested as 3 components. For these selections of major components, the high explained variations for P17 and NOX strains reached individual values of 93.68% and 93.64%, respectively. Furthermore, the percentage of residual decrease reached a maximal value. Similar situations occurred for both acetate substrate conditions while 3 major metabolic components were selected for both the P17 and NOX strains.

As for the verification of the results obtained with the PARAFAC model, three kinds of acetate concentration were achieved by split-half experiments using a test of  $S_4C_4T_2$  (Splits: 4, Combinations: 4, Tests: 2); however, only the substrate of 100  $\mu\text{g}$  acetate-C/L is plotted in Fig. 1 owing to the limitation of content. The results from Fig. 1 show that similar curves for each pair of halves based on the split half analysis further validated that utilizing three components was appropriate for characterizing the metabolic fluorescence property from both strains. Regarding the deviations of the sum of squares located at 400 nm Ex and 450 nm Em for the P17 strain, similar phenomena were found in the location of protein-like species, owing to the varied emission spectra across different samples [40]. Murphy et al. [14] further explained that the similarity of split modeling might be affected by the numbers and sources of the samples.

### 3.2. Major components of metabolic organic matter during P17 strains cultivation

In this study, a control test without addition of acetate-C was designed as a comparative experiment with the additions of 10 and 100  $\mu\text{g}$  acetate-C/L. Hence, for the application of FEEM + PARAFAC for the determination of FDOM released from bacterial strains, the control test should be excluded and independently analyzed. According to the report of Goto et al. [41], when a marine bacterial isolate, *Alteromonas macleodii*, was grown in glucose (1 mmol C L<sup>-1</sup>), DOM produced by the strain exhibited five fluorescent peaks during the processes of growth, indicating that the metabolic organic matter from both strains in the AOC bioassay may be affected by the 10-fold difference in concentration. Furthermore, Helbling et al. [42] proved that substrate utilization kinetics could be affected by substrate concentration. Based on the previous description, the application of FEEM + PARAFAC to bacterial FDOM released from both strains grown in three acetate-C concentrations are individually analyzed and compared.

After the decision of metabolic component numbers, the maximum fluorescence intensities (FI) of the individual components could be used as their relative concentrations or

contents. The FI percentage, calculated by the FI of each component to the total FI of whole components (e.g., P1%, P2%, and P3%) was considered as the contribution of individual chemical composition. The diagrams of major metabolic components from P17 strains grown in the control test, 10, and 100  $\mu\text{g}$  acetate-C/L are, respectively, shown in Fig. 2. The locations of Ex/Em wavelengths and the properties of metabolic organic matter from the P17 strain were thoroughly listed in Table 2.

As shown in Fig. 2a and listed in Table 2, the duration of the P17 strain growth control test without the addition of acetate concentration had 3 components including: P1<sub>control</sub> with the primary peak at 230/300 nm (Ex/Em) belonging to tyrosine-like substances [43]; P2<sub>control</sub> with 280/330 nm belonging to tryptophan-like substances [44], and P3<sub>control</sub> with the longest excitation/emission wavelengths of 410/460 nm belonging to humic-like substances [39]. The percentages of P1<sub>control</sub>, P2<sub>control</sub>, and P3<sub>control</sub> were, respectively, 46.9%, 29.72% and 17%, indicating that metabolic organic matter is dominated by protein composition; without acetate addition, the P17 strain could continuously utilize the original organic matter.

The P1<sub>10</sub> components of metabolic organic content from the P17 strain incubated with 10  $\mu\text{g}$  acetate-C/L, shown in Table 2, were located at 230/330 nm and 280/330 nm, respectively, attributed to tyrosine and tryptophan-like substances. The P2<sub>10</sub> component of 270/420 nm may be related with humic-like substances [45]. The P3<sub>10</sub> component of 410/460 nm were the same as the P3<sub>control</sub>. Regarding the variation of the FI percentages of each component, P1<sub>10</sub>, P2<sub>10</sub>, and P3<sub>10</sub> metabolic organic matter from the P17 strain incubated with 10  $\mu\text{g}$  acetate-C/L, produced values of 66.03%, 17.35%, and 11.65%, respectively, indicating that a new substance at 270/420 nm was formed while in the 10  $\mu\text{g}$ -acetate-C/L condition as compared with the control test. The humus content increased from 17% in the control test to 29% in 10  $\mu\text{g}$ -acetate-C/L, while the protein content decreased from 76.68% in the blank test to 66.03% in 10  $\mu\text{g}$ -acetate-C/L.

Interestingly, the order of major components of P17 grown in 100  $\mu\text{g}$  acetate-C/L, shown in Fig. 2c and listed in Table 2, exhibited a variation in comparison with the P17 strain grown in the control test and 10  $\mu\text{g}$  acetate-C/L. The P1<sub>100</sub> component detected at 230/330 nm was characterized as tyrosine-like substance, and the 280/330 nm reading was attributed to tryptophan-like substance. The P2<sub>100</sub> component at 410/460 nm was classified as humic-like substance. The P3<sub>100</sub> detection at 230/300 nm was attributed to tyrosine-like substance. The percentages of metabolic organic content in P1<sub>100</sub>, P2<sub>100</sub> and P3<sub>100</sub> from the P17 strain incubated with 100  $\mu\text{g}$  acetate-C/L were 41.6%, 31.93%, and 21.51%, respectively, this revealed that 31.93% of humus content become more attributed to metabolic organic matter than the 29% of humus content in 10  $\mu\text{g}$  acetate-C/L, or even 17% of humus content in the control test. Of course, regarding both the 230/330 nm and 280/330 nm components, their contents decreased from 66.03% in 10  $\mu\text{g}$  acetate-C/L to 41.46% in 100  $\mu\text{g}$  acetate-C/L. Interestingly, the 270/420 nm signal attributed to humic-like substance did not appear in 100  $\mu\text{g}$  acetate-C/L. This result revealed that the composition and content from the P17 strain may be affected by the content of acetate addition.

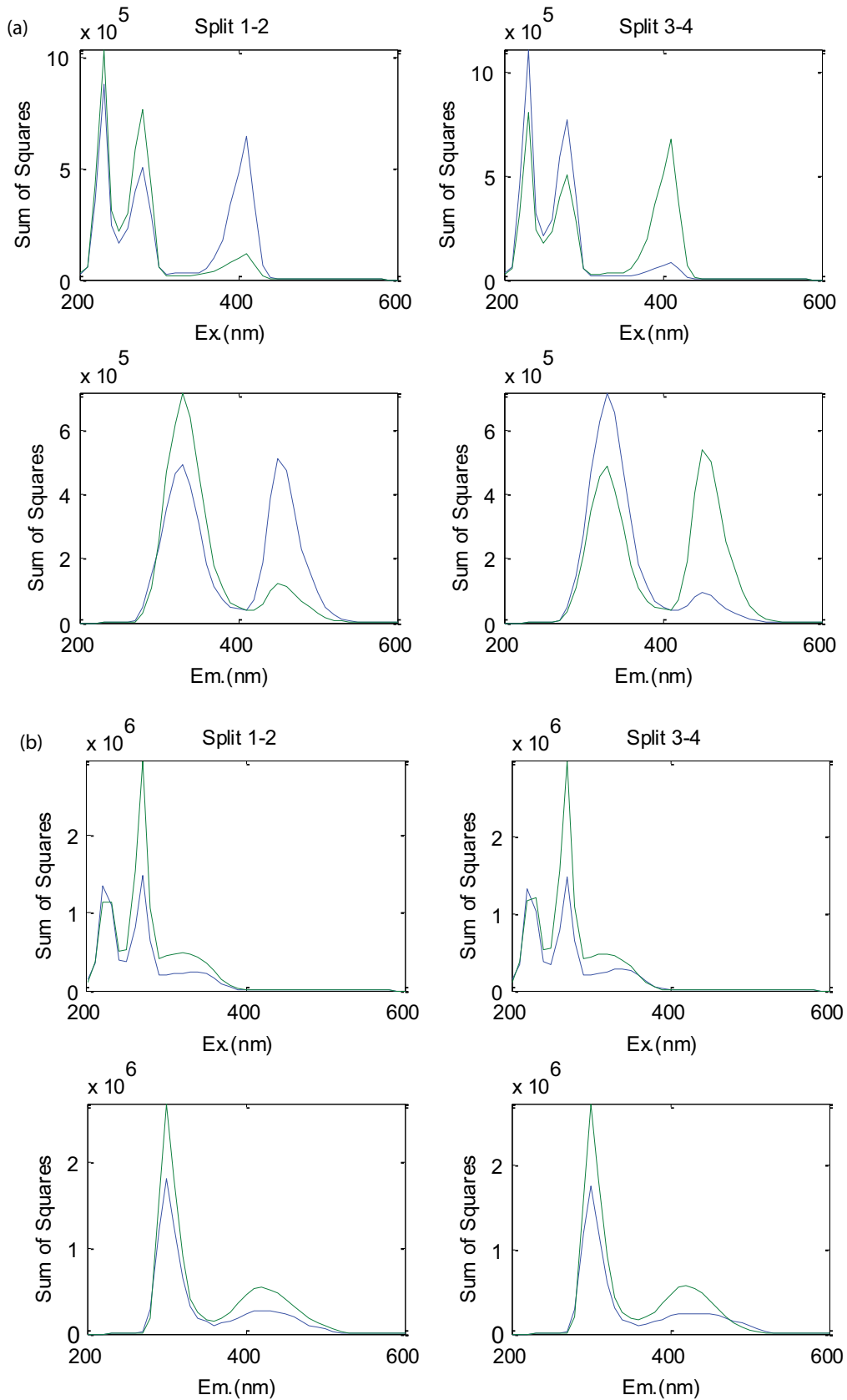


Fig. 1. Split half validation of metabolic organic FEEM from (a) P17 and (b) NOX strains (with the addition of 100 µg acetate-C/L; the other acetate substrates are not shown in this research).

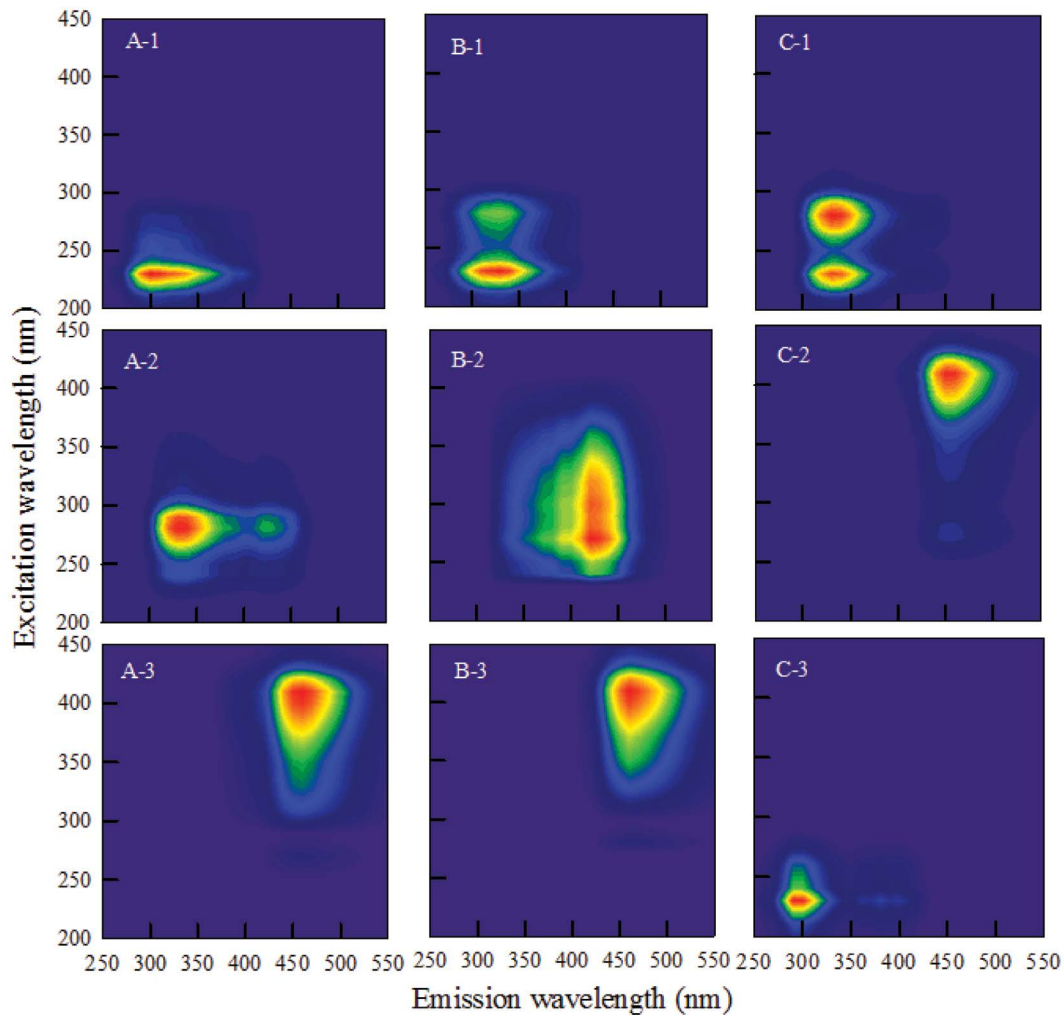


Fig. 2. Major metabolic components of the P17 strain grown in the acetate concentrations of (a) control, (b) 10, and (c) 100  $\mu\text{g}$  acetate-C/L by FEEM + PARAFAC. (1) P1, (2) P2 and (3) P3; their EX/EM locations are described in Table 2; ( $N = 6$ ).

### 3.3. Major components of metabolic organic matter during NOX strain cultivation

Regarding the major components of metabolic organic matter from the NOX strain, their diagrams of FEEM + PARAFAC, locations of excitation and emission wavelengths and characteristics are illustrated in Fig. 3 and listed in Table 3. For the control test, as shown in Fig. 3a and listed in Table 3, the reading at 340/440 nm of the  $N1_{\text{control}}$  was classified as a humic-like substance [46]. Both compositions of  $N2_{\text{control}}$  components included the 220/300 nm and 270/300 nm signals, respectively, belonging to tyrosine-like substance [44]. Both substances at 240/410 nm and 300/410 nm existing in the  $N3_{\text{control}}$  component belonged to humic-like substance [39]. The percentages of  $N1_{\text{control}}$ ,  $N2_{\text{control}}$  and  $N3_{\text{control}}$  were respectively 34.83%, 33.56% and 25.26%, indicating the presence of 60.09% humic-like substance protein, which is higher than the 33.56% of protein-like substance without acetate addition composition; these results are the opposite of the results for the P17 strain.

Regarding the NOX strain grown in the condition of 10  $\mu\text{g}$  acetate-C/L, the diagrams of FEEM + PARAFAC, locations of

excitation and emission wavelengths and characteristics are illustrated in Fig. 3b and listed in Table 3. The  $N1_{10}$  component, with the 220/300 nm signal belonging to a tyrosine-like substance and that at 270/300 nm belonging to a tyrosine-like substance [44], was classified as organic matter containing nitrogen. The  $N2_{10}$  component included 340/440 nm, which was attributed to the humic-like substance. Both compositions of 240/410 nm and 300/410 nm in the  $N3_{10}$  component belonged to the humic-like substance. The percentages of  $N1_{10}$ ,  $N2_{10}$  and  $N3_{10}$  were 45.04%, 27.74%, and 20.61%, respectively, indicating presence of 48.35% humic-like substance, which was less than the 59.09% of the control test; this is owing to the increase of organic matter containing that contains nitrogen in the condition of 10  $\mu\text{g}$  acetate-C/L in comparison with the control test.

For the NOX strain grown in the condition of 100  $\mu\text{g}$  acetate-C/L, the diagrams of FEEM + PARAFAC are shown in Fig. 3c, and the locations of excitation and emission wavelengths and the characteristics of three components are listed in Table 3. The  $N1_{100}$  component exhibited both peak locations of 230/300 nm and 270/300 nm, respectively, and

Table 2  
Summary of metabolic organic components from P17 strains incubated with different acetate concentrations (N = 6 for each substrate concentration)

Metabolic organic Components	Incubated with $\mu\text{g}$ acetate-C/L			Ex/Em' nm	Description	References
	Control	10	100			
P1	230/300	230/330	230/330	230/300	Tyrosine-like	[43]
	(46.96%)**	280/330	280/330	230/330	Tryptophan-like	[43]
		(66.03%)	(41.46%)	280/330	Tryptophan-like	[44]
P2	280/330	270/420	410/460	280/330	Tryptophan-like	[44]
	(29.72%)	(17.35%)	(31.93%)	270/420	Humic-like	[45]
				410/460	Humic-like	[39]
P3	410/460	410/460	230/300	230/330	Tryptophan-like	[43]
	(17.00%)	(11.65%)	(21.51%)	410/460	Humic-like	[39]

\*EX/EM: Excitation/Emission wavelengths.

\*\*The percentage of FI of each component to the total FI of whole components.

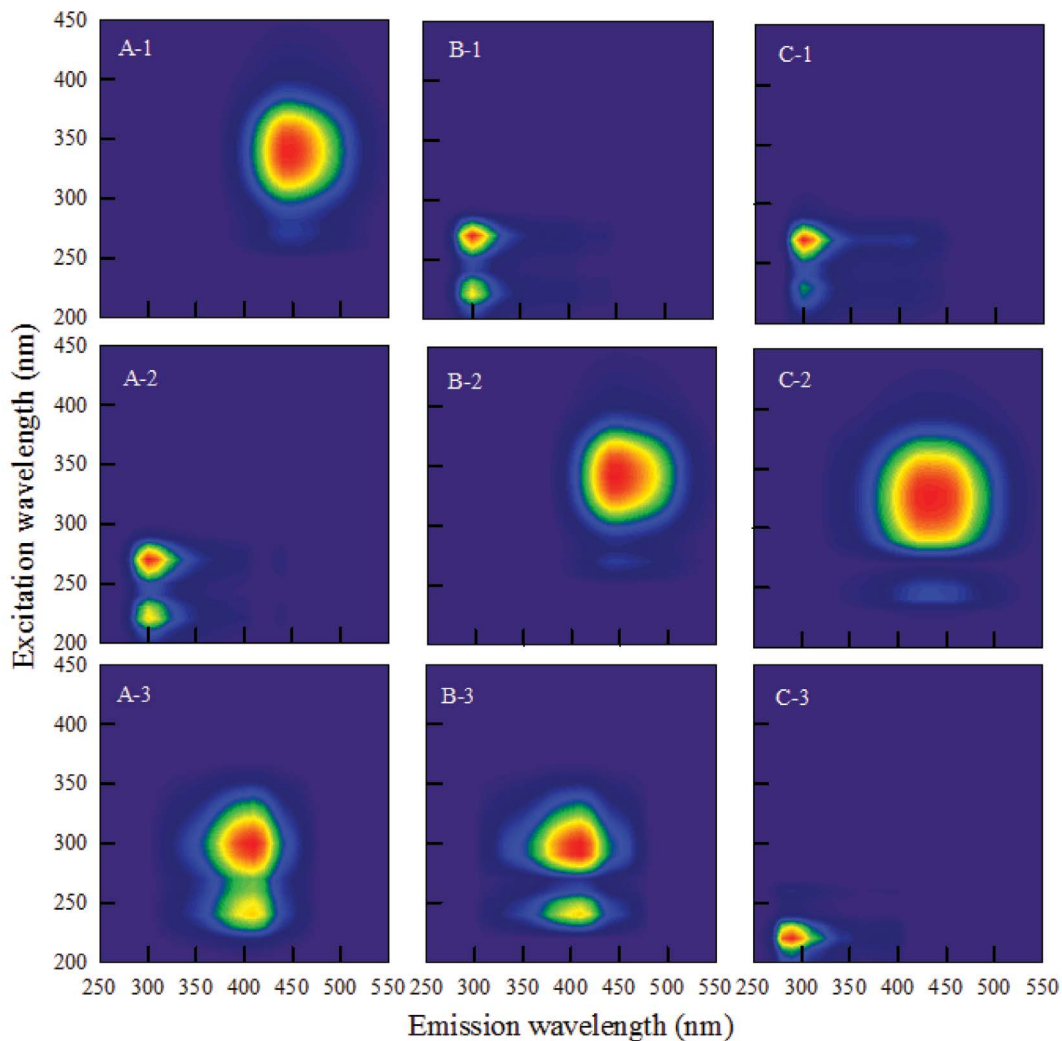


Fig. 3. Major metabolic components of the NOX strain grown in the acetate concentrations of (a) control, (b) 10, and (c) 100  $\mu\text{g}$  acetate-C/L by FEEM + PARAFAC. (1) N1, (2) N2 and (3) N3; their EX/EM locations are described in Table 2; (N = 5).

Table 3

Summary of metabolic organic components from NOX strains incubated with different acetate concentrations ( $N = 5$  for each substrate concentration)

Metabolic organic components	Incubated with $\mu\text{g}$ acetate-C/L			Ex/Em* nm	Description	References.
	Control	10	100			
N1	340/440	220/300	230/300	220/300	Tyrosine-like	[44]
	(34.83%)**	270/300	270/300	230/300	Tyrosine-like	[43]
		(45.04%)	(42.32%)	270/300	Tyrosine-like	[44]
				340/440	Humic-like	[46]
N2	220/300	340/440	330/440	220/300	Tyrosine-like	[44]
	270/300	(27.74%)	(32.03%)	270/300	Tyrosine-like	[44]
	(33.56%)			330/440	Humic-like	[46]
				340/440	Humic-like	[46]
N3	240/410	240/410	220/290	220/290	Tyrosine-like	[44]
	300/410	300/410	(18.73%)	240/410	Humic-like	[39]
	(25.26%)	(20.61%)		300/410	Humic-like	[39]

\*EX/EM: Excitation/Emission wavelengths.

\*\*The percentage of FI of each component to the total FI of whole components.

were attributed to tyrosine-like substance [44].  $N2_{100}$  owned the primary peak location of 330/440 nm, belonging to humic-like substance [46]. Only one composition of  $N3_{100}$  was located at 220/290 nm, which was classified as tyrosine-like substance [44].

The percentages of  $N1_{100}$ ,  $N2_{100}$  and  $N3_{100}$  of metabolic organic content from the NOX strain incubated with 100  $\mu\text{g}$  acetate-C/L were, respectively, 42.32%, 32.03%, and 18.73%, revealing that more humic-like substance located at 330/440 nm in 100  $\mu\text{g}$  acetate-C/L was observed than in the condition with 10  $\mu\text{g}$  acetate-C/L; however, both 240/410 nm and 310/410 nm, which belonging to humic-like substance in 10  $\mu\text{g}$  acetate-C/L, disappeared in 100  $\mu\text{g}$  acetate-C/L. Apparently, the composition and percentage of humic-like substance from the NOX strain is affected by the addition of acetate concentration. Similar phenomena are observed in metabolic organic matter from the P17 strain.

#### 3.4. Integrated analysis concerning in major metabolic components between P17 and NOX strains

Actually, researchers had previously proven that peak A (~225 nm/400–500 nm), peak C (300–350 nm/400–500 nm) peak M (310–320 nm/380–420 nm), peak T (~225 (~280)/~350 nm), peaks T1 of 275/340 nm and T2 of 225–235/340–360 nm, and peak B (~225 (~280)/~305 nm) possibly resulted from living and dead cellular material in addition to their exudates from anthropogenic activities [47,48].

In comparison with the control test in Tables 2 and 3, the FI percentage of metabolic organic matter containing nitrogen from P17 was superior to the metabolic humic-like substance; in contrast, the FI percentage of metabolic humic-like organic matter from the NOX strain far exceeded those of the metabolic protein-like and tyrosine-like substances containing nitrogen. For the metabolic organic matter from both P17 and NOX strains, the composition and FI

percentage of metabolic organic matter containing nitrogen and humic-like substance varied with the addition of acetate concentration.

Apparently, regarding the differences of FI percentages of major metabolic components between the P17 and NOX strains at different acetate concentrations, two possible explanations were reasonable, including the direct production during bacterial biosynthesis and growth, and the production of byproducts during bacterial biodegradation of DOM, such as the conformational changes of the ambient DOM [49]. Furthermore, in actuality, fluorescent protein-like products could be produced by the viral lysis of bacteria [50].

#### 4. Conclusions

The main conclusions of this study include the followings:

- Metabolic organic matter from both P17 and NOX strains could be evaluated by the selection of three components based on the integrated consideration including core consistency, residuals, and split-half experiments, especially for over 93% of explained variations.
- For the control test, the characteristic of metabolic organic matter from the P17 strain was different with that from NOX strain, fluorescent intensity belonging to the humic-like substances from the P17 strain was less than that from the NOX strain.
- The FI percentage of protein-like substance released from the P17 strain at emission wavelength less than 330 nm was decreased with escalating acetate concentration.
- The FI percentage of metabolic organic matter belonging to the humic-like substance class from the NOX strain decreased with the ascending acetate concentrations. Moreover, humic-like substances at 410 nm emission wavelength disappeared in 100  $\mu\text{g}$  acetate-C/L while

the 220/290 nm of emitting substance was classified as nitrogen-containing protein appearing in the substrate concentration.

- The composition and FI percentage of metabolic organic matter containing nitrogen and humic-like substances varied with the addition of acetate concentrations.

### Acknowledgement

This project was funded in part by the Ministry of Science and Technology, Taiwan (Contract Number: MOST 106-2221-E-127-001 & MOST 107-2221-E-127-001-MY2). The authors would like to thank the personnel at the Ministry of Science and Technology for the assistance and support throughout this project.

### References

- [1] E.I. Prest, F. Hammes, M.C.M. van Loosdrecht, J.S. Vrouwenvelder, Biological stability of drinking water: controlling factors, methods, and challenges, *Front. Microbiol.*, 7 (2016) 1–24.
- [2] S. Aggarwal, Y. Jeon, R.M. Hozalski, Feasibility of using a particle counter or flow-cytometer for bacterial enumeration in the assimilable organic carbon (AOC) analysis method, *Biodegradation*, 26 (2015) 387–397.
- [3] L.G. Terry, R.S. Summers, Biodegradable organic matter and rapid-rate biofilter performance: a review, *Water Res.*, 128 (2018) 234–245.
- [4] M. LeChevallier, Measurement of Biostability and Impacts on Water Treatment in the US, *Microbial Growth in Drinking Water Supplies*, IWA Publishing, London, 2014, pp. 33–56.
- [5] W. Li, J. Zhang, F. Wang, L. Qian, Y. Zhou, W. Qi, J. Chen, Effect of disinfectant residual on the interaction between bacterial growth and assimilable organic carbon in a drinking water distribution system, *Chemosphere*, 202 (2018) 586–597.
- [6] E.H. Goslan, C. Seigle, D. Purcell, R. Henderson, S.A. Parsons, B. Jefferson, S.J. Judd, Carbonaceous and nitrogenous disinfection by-product formation from algal organic matter, *Chemosphere*, 170 (2017) 1–9.
- [7] M. Sillanpää, Characterization of (NOM) Natural Organic Matter in Water: Characterization and Treatment Methods, Heinemann, Butterworth, Oxford, 2015, pp. 17–54.
- [8] Y. Xu, T. Chen, Z. Liu, S. Zhu, F. Cui, W. Shi, The impact of recycling alum-humic-floc (AHF) on the removal of natural organic materials (NOM): behavior of coagulation and adsorption, *Chem. Eng. J.*, 284 (2016) 1049–1057.
- [9] Q. Zheng, X. Yang, W. Deng, X.C. Le, X.F. Li, Characterization of natural organic matter in water for optimizing water treatment and minimizing disinfection by-product formation, *J. Environ. Sci.*, 42 (2016) 1–5.
- [10] A. Matilainen, E.T. Gjessing, T. Lahtinen, L. Hed, A. Bhatnagar, M. Sillanpää, An overview of the methods used in the characterisation of natural organic matter (NOM) in relation to drinking water treatment, *Chemosphere*, 83 (2011) 1431–1442.
- [11] Y. Shatoya, A. Baker, J. Bridgeman, R.K. Henderson, On-line monitoring of organic matter concentrations and character in drinking water treatment systems using fluorescence spectroscopy, *Environ. Sci. Water Res. Technol.*, 2 (2016) 749–760.
- [12] Y. Shutova, A. Baker, J. Bridgeman, R.K. Henderson, Spectroscopic characterisation of dissolved organic matter changes in drinking water treatment: from PARAFAC analysis to online monitoring wavelengths, *Water Res.*, 54 (2014) 159–169.
- [13] D.M. Golea, A. Upton, P. Jarvis, G. Moore, S. Sutherland, S.A. Parsons, S.J. Judd, THM and HAA formation from NOM in raw and treated surface waters, *Water Res.*, 112 (2017) 226–235.
- [14] K.R. Murphy, C.A. Stedmon, D. Graeber, R. Bro, Fluorescence spectroscopy and multi-way techniques. PARAFAC, *Anal. Methods*, 5 (2013) 6557–6566.
- [15] A. Stubbins, J.F. Lapierre, M. Berggren, Y.T. Prairie, T. Dittmar, P.A. del Giorgio, What's in an EEM? Molecular signatures associated with dissolved organic fluorescence in Boreal Canada, *Environ. Sci. Technol.*, 48 (2014) 10598–10606.
- [16] A. Baker, S.A. Cumberland, C. Bradley, C. Buckley, J. Bridgeman, To what extent can portable fluorescence spectroscopy be used in the real-time assessment of microbial water quality?, *Sci. Total Environ.*, 532 (2015) 14–19.
- [17] J.P. Ritson, N.J.D. Graham, M.R. Templeton, J.M. Clark, R. Gough, C. Freeman, The impact of climate change on the treatability of dissolved organic matter (DOM) in upland water supplies: a UK perspective, *Sci. Total Environ.*, 473–474 (2014) 714–730.
- [18] K.M.H. Beggs, R.S. Summers, Character and chlorine reactivity of dissolved organic matter from a mountain pine beetle impacted watershed, *Environ. Sci. Technol.*, 45 (2011) 5717–5724.
- [19] M. Vera, S. Cruz, M.R. Boleda, J. Mesa, J. Martín-Alonso, S. Casas, O. Gibert, J.L. Cortina, Fluorescence spectroscopy and parallel factor analysis as a dissolved organic monitoring tool to assess treatment performance in drinking water trains, *Sci. Total Environ.*, 584–585 (2017) 1212–1220.
- [20] P.G. Coble, Characterization of marine and terrestrial DOM in seawater using excitation-emission matrix spectroscopy, *Mar. Chem.*, 51 (1996) 325–346.
- [21] W. Chen, P. Westerhoff, J.A. Leenheer, K. Booksh, Fluorescence excitation–emission matrix regional integration to quantify spectra for dissolved organic matter, *Environ. Sci. Technol.*, 37 (2004) 5701–5710.
- [22] T. Persson, M. Wedborg, Multivariate evaluation of the fluorescence of aquatic organic matter, *Anal. Chim. Acta*, 434 (2001) 179–192.
- [23] C. Qian, L.F. Wang, W. Chen, Y.S. Wang, X.Y. Liu, H. Jiang, H.Q. Yu, Fluorescence approach for the determination of fluorescent dissolved organic matter, *Anal. Chem.*, 89 (2017) 4264–4271.
- [24] J.H. Goldman, S.A. Rounds, J.A. Needoba, Applications of fluorescence spectroscopy for predicting percent wastewater in an urban stream, *Environ. Sci. Technol.*, 46 (2012) 4374–4381.
- [25] L. Yang, J. Hur, W. Zhuang, Occurrence and behaviors of fluorescence EEM-PARAFAC components in drinking water and wastewater treatment systems and their applications: a review, *Environ. Sci. Pollut. Res.*, 22 (2015) 6500–6510.
- [26] R.K. Henderson, A. Baker, K.R. Murphy, A. Hambly, R.M. Stuetz, S.J. Khan, Fluorescence as a potential monitoring tool for recycled water systems: a review, *Water Res.*, 43 (2009) 863–881.
- [27] R. Bro, M. Vidal, EEMizer: automated modeling of fluorescence EEM data, *Chemom. Intell. Lab. Syst.*, 106 (2011) 86–92.
- [28] S.A. Bagtho, S.K. Sharma, G.L. Amy, Tracking natural organic matter (NOM) in a drinking water treatment plant using fluorescence excitation–emission matrices and PARAFAC, *Water Res.*, 45 (2011) 797–809.
- [29] M. Esparza-Soto, S. Núñez-Hernández, C. Fall, Spectrometric characterization of effluent organic matter of a sequencing batch reactor operated at three sludge retention times, *Water Res.*, 45 (2011) 6555–6563.
- [30] K.R. Murphy, A. Hambly, S. Singh, R.K. Henderson, A. Baker, R. Stuetz, S.J. Khan, Organic matter fluorescence in municipal water recycling schemes: toward a unified PARAFAC model, *Environ. Sci. Technol.*, 45 (2011) 2909–2916.
- [31] C.L. Osburn, C.A. Stedmon, Linking the chemical and optical properties of dissolved organic matter in the Baltic–North Sea transition zone to differentiate three allochthonous inputs, *Mar. Chem.*, 126 (2011) 281–294.
- [32] C.A. Stedmon, B. Sereďynska-Sobecka, R. Boe-Hansen, N. Le Tallec, C.K. Waul, E. Arvin, A potential approach for monitoring drinking water quality from groundwater systems using organic matter fluorescence as an early warning for contamination events, *Water Res.*, 45 (2011) 6030–6038.

- [33] P.A. Staehr, L. Baastrup-Spohr, K. Sand-Jensen, C. Stedmon, Lake metabolism scales with lake morphometry and catchment conditions, *Aquat. Sci.*, 74 (2012) 155–169.
- [34] E. Cohen, G.J. Levy, M. Borisover, Fluorescent components of organic matter in wastewater: efficacy and selectivity of the water treatment, *Water Res.*, 55 (2014) 323–334.
- [35] D. Van der Kooij, H. Veenendaal, Determination of the Concentration of Easily Assimilable Organic Carbon (AOC) in Drinking Water With Growth Measurement Using Pure Bacterial Cultures, KIWA NV, 1995.
- [36] R. Bro, PARAFAC. Tutorial and applications, *Chemometr. Intell. Lab.*, 38 (1997) 149–171.
- [37] C.A. Stedmon, R. Bro, Characterizing dissolved organic matter fluorescence with parallel factor analysis: a tutorial, *Limnol. Oceanogr. Methods*, 6 (2008) 572–579.
- [38] K. Shimotori, K. Watanabe, T. Hama, Fluorescence characteristics of humic-like fluorescent dissolved organic matter produced by various taxa of marine bacteria, *Aquat. Microb. Ecol.*, 65 (2012) 249–260.
- [39] S.K.L. Ishii, T.H. Boyer, Behavior of Reoccurring PARAFAC components in fluorescent dissolved organic matter in natural and engineered systems: a critical review, *Environ. Sci. Technol.*, 46 (2012) 2006–2017.
- [40] W.T. Li, S.Y. Chen, Z.X. Xu, Y. Li, C.D. Shuang, A.M. Li, Characterization of dissolved organic matter in municipal wastewater using fluorescence PARAFAC analysis and chromatography multi-excitation/emission scan: a comparative study, *Environ. Sci. Technol.*, 48 (2014) 2603–2609.
- [41] S. Goto, Y. Tada, K. Suzuki, Y. Yamashita, Production and reutilization of fluorescent dissolved organic matter by a marine bacterial strain, *Alteromonas macleodii*, *Front. Microbiol.*, 8 (2017) 1–10.
- [42] D.E. Helbling, F. Hammes, T. Egli, H.-P.E. Kohler, Kinetics and yields of pesticide biodegradation at low substrate concentrations and under conditions restricting assimilable organic carbon, *Appl. Environ. Microbiol.*, 80 (2014) 1306–1313.
- [43] Y. Zhou, K. Shi, Y. Zhang, E. Jeppesen, X. Liu, Q. Zhou, H. Wu, X. Tang, G. Zhu, Fluorescence peak integration ratio  $I_C: I_T$  as a new potential indicator tracing the compositional changes in chromophoric dissolved organic matter, *Sci. Total Environ.*, 574 (2017) 1588–1598.
- [44] H. Xu, H. Cai, G. Yu, H. Jiang, Insights into extracellular polymeric substances of cyanobacterium *Microcystis aeruginosa* using fractionation procedure and parallel factor analysis, *Water Res.*, 47 (2013) 2005–2014.
- [45] Y. Yuan, B. Xi, X. He, W. Tan, R. Gao, H. Zhang, C. Yang, X. Zhao, C. Huang, D. Li, Compost-derived humic acids as regulators for reductive degradation of nitrobenzene, *J. Hazard. Mater.*, 339 (2017) 378–384.
- [46] F. Qu, H. Liang, Z. Wang, H. Wang, H. Yu, G. Li, Ultrafiltration membrane fouling by extracellular organic matters (EOM) of *Microcystis aeruginosa* in stationary phase: influences of interfacial characteristics of foulants and fouling mechanisms, *Water Res.*, 46 (2012) 1490–1500.
- [47] J. Bridgeman, A. Baker, C. Carliell-Marquet, E. Carstea, Determination of changes in wastewater quality through a treatment works using fluorescence spectroscopy, *Environ. Technol.*, 34 (2013) 3069–3077.
- [48] H. Yu, Y. Song, R. Liu, H. Pan, L. Xiang, F. Qian, Identifying changes in dissolved organic matter content and characteristics by fluorescence spectroscopy coupled with self-organizing map and classification and regression tree analysis during wastewater treatment, *Chemosphere*, 113 (2014) 79–86.
- [49] C.A. Stedmon, R.M. Cory, Biological Origins and Fate of Fluorescent Dissolved Organic Matter in Aquatic Environments, P.G. Coble, J. Lead, A. Baker, D.M. Reynolds, R.G. Spencer, Eds., *Aquatic Organic Matter Fluorescence*, Cambridge University Press, Cambridge, 2014, pp. 278–299.
- [50] R.A. Sipler, D.A. Bronk, Dynamics of Dissolved Organic Nitrogen, D.A. Hansell, C.A. Carlson, *Biogeochemistry of Marine Dissolved Organic Matter*, Academic Press, Waltham, 2015, pp. 128–232.